Surface superconductivity on Weyl semimetal induced by nonmagnetic and ferromagnetic tips

Jiawei Luo,[1] Yanan Li,[1,2] Jiachen Li,[1] Tatsuki Hashimoto,[3] Takuto Kawakami,[3] Hong Lu,[1] Shuang Jia,[1] Masatoshi Sato,[3] and Jian Wang[1,4,5,6,*]

[1]*International Center for Quantum Materials, School of Physics, Peking University, Beijing 100871, China*
[2]*Department of Physics, Pennsylvania State University, University Park, Pennsylvania 16802, USA*
[3]*Yukawa Institute for Theoretical Physics, Kyoto University, Kyoto 606–8502, Japan*
[4]*Collaborative Innovation Center of Quantum Matter, Beijing 100871, China*
[5]*CAS Center for Excellence in Topological Quantum Computation, University of Chinese Academy of Sciences, Beijing 100190, China*
[6]*Beijing Academy of Quantum Information Sciences, Beijing 100193, China*

(Received 18 March 2019; published 6 December 2019)

Topological superconductors showing Majorana fermions or bound states at the edge or surface are promising components for potential quantum computation and thus attract much attention in physical sciences. Recently, topological Weyl fermion states have been discovered in nonsuperconducting TaP crystals, which may offer a great platform to investigate topological nontrivial superconductivity if superconductivity can be induced wherein. Here we report the discovery of nonmagnetic and ferromagnetic tips induced unconventional interface superconductivity around the nanoscale point contact region on TaP crystals. The tip-induced superconductivity (TISC) at the contact is enhanced with the ferromagnetic Ni tip, comparing with nonmagnetic Au and PtIr tips. The point contact spectroscopy shows evidences of anisotropic superconductivity with the mixed spin-triplet pairing, indicating unconventional superconducting nature. Moreover, the Shubnikov–de Haas oscillations in magnetoresistance are detected from the tip-point-contact measurement, which demonstrate that the nonzero Berry phase or topological nontrivial property of TaP maintains under the tip point contact. The theoretical analysis shows that surface superconductivity plays a major role in this TISC and there exists a large spin-triplet mixing in the gap function. Therefore, our work suggests an intriguing Weyl surface superconducting state on TaP.

DOI: 10.1103/PhysRevMaterials.3.124201

I. INTRODUCTION

Recent discovery of topological Weyl semimetals (WSMs) is a breakthrough in condensed matter physics [1–6]. For WSMs, the bulk electronic bands disperse linearly along momentum directions through the Weyl point and the surface states are topologically protected Fermi arcs connecting the Weyl nodes with opposite chirality. Among them, TaP has been theoretically and experimentally proven to be a time reversal symmetry protected but inversion symmetry broken Weyl semimetal [7,8] without any toxic elements. Some quantum phenomena like negative magnetoresistance, unsaturated large positive magnetoresistance, ultrahigh mobility charge carriers, and magnetic-tunneling-induced Weyl node annihilation have been observed in TaP [9–13]. Although TaP is not a superconductor, under high pressure of 30 GPa, TaP can show superconductivity of 3.07 K with a structure phase transition [14]. However, it is hard to characterize topological properties by such high pressure techniques. The point contact spectroscopy (PCS) technique plays an important role in the history of determining the pairing symmetries and gap energy of superconductors [15], among the most representative are the *p*-wave candidate Sr_2RuO_4 [16], two-band MgB_2 [17], *d*-wave $YBa_2Cu_3O_{7-\delta}$ [18], heavy-fermion $CeCoIn_5$ [19], and topological superconductor candidate $Cu_xBi_2Se_3$ [20]. The PCS is usually conducted on normal metal/superconductor junctions and shows the nonlinearity of the normalized *dI/dV* versus junction voltage, where the applied voltage defines the energy scale for the superconducting order parameter. Point contacts (PCs) have mainly been carried out in two different configurations, the hard PC method and the soft PC method. The most often used is the so-called "needle-anvil" hard PC method by bringing a metallic tip on the sample to form a junction. This unique method may bring pressure, doping or interface effects on the sample surface, which need to be avoided in the study of intrinsic superconductors. However, these additional effects could also provide a promising route to modulating sample properties and achieving quantum states [21,22] like traditional high pressure and gating techniques. Recently, superconductivity was successfully induced in topological semimetals Cd_3As_2 single crystals [23] and polycrystals [24], as well as TaAs [25,26] via the tip-point-contact technique. Furthermore, tip enhanced superconductivity was also detected in topological nontrivial Au_2Pb crystals [27].

In this paper, we report the TISC on the surface of noncentrosymmetric Weyl semimetal TaP by PC method. The TISC spectroscopy results of TaP sample I (S1) and sample II (S2) are detected by both nonmagnetic Au/PtIr tips and ferromagnetic Ni tip. By using nonsuperconducting tips, the spectra on most positions and different samples consistently show an onset superconducting transition temperature (T_c^{onset}) from 1 to 3 K, reminiscent of pressure results on TaP [14]. The observed double conductance peaks are consistent with

*jianwangphysics@pku.edu.cn

the typical features of the nonzero energy Andreev bound state (ABS), indicating unconventional superconductivity. More interestingly, when using a ferromagnetic Ni tip, superconductivity can still be induced around the nanoscale point contact interface on nonsuperconducting TaP and the T_c^{onset} is even higher (larger than 5 K) with a larger superconducting gap. The observation further excludes the possibility of conventional superconductivity and suggests the mixed spin-triplet and spin-singlet Cooper pairing of noncentrosymmetric Weyl semimetal TaP. The topological properties remain at the point contact region on TaP crystals according to the analysis of quantum oscillations. The superconducting states mentioned above are all repeatable and our theoretical analysis suggests the surface superconductivity with spin-triplet and spin-singlet mixing is induced by the tips on Weyl semimetals.

II. METHODS

The single crystals of TaP are grown using chemical vapor transport technique as described in Refs. [9] and [11]. The bulk magnetoresistance are obtained by standard four-electrode electrical transport measurement in a 16T-Quantum Design physical property measurement system (PPMS-Model 6000). A mechanically sharpened tip is utilized to be perpendicularly pushed onto the sample to form a junction as the hard point contact method in our measurements. The hard point contact is exerted on the *ab* plane of a TaP single crystal. The size of the tip is around 1 μm as seen from the microscope and the size of the effective contacting area is in the scale of 0.1 μm or less. The resistance between the tip and sample, namely point contact resistance, is usually in the range of 5–40 Ω. Actually a single contact point consists of numerous subjunctions with nanometer size in a micro scheme and the interface between the tip and TaP sample forms a barrier. The strength of the barrier is usually denoted as a parameter Z, which takes into consideration the oxidation of the interface, mismatch of the wave vector of tip and TaP sample, and so on.

The sample TaP and thermometer RX102a are glued on a copper sample holder electrically isolated by GE varnish. The sample holder is fixed onto an attocube nanopositioner stack so that the position of the sample can be precisely controlled. The tip is fixed on a copper tip holder to ensure that the tip would also be cooled down to ultralow temperature. Both the stack and the tip holder are mounted onto a cooper frame that is suspended with BeCu springs at the bottom of a probe insertable for a Leiden dilution refrigerator (CF450). After adjusting the sample position to the field center of the vector magnet, magnetic field 3 T in the z direction, 1 T in x, and 1 T in the y direction could be applied.

The differential resistance dV/dI of the PC is measured with standard lock-in technique and the normalized differential conductance $(dI/dV)_n$ is the differential conductance $(dI/dV = 1/(dV/dI))$ normalized by a normal state differential conductance at the high bias.

III. RESULTS

As shown in Fig. 1(a), the temperature dependence of the standard four-electrode resistance of S1 at zero field (blue curve) exhibits metallic like behavior with no sign of superconductivity. Figure 1(b) shows the temperature dependence of the point contact resistance at zero field (blue curve) and 3 T (green curve), respectively. The PC resistance at zero field remains constant at temperature above 3.0 K and drops there after. The resistance drop results from the Andreev reflection process and disappears at 3 T, indicating the TISC around the point contact region can be suppressed by the applied magnetic field of 3 T. Note that the PC resistance for a superconductor can never become zero as it contains the Sharvin resistance ($R_s = 16R_q/(k_F d)^2$, where $R_q = h/2e^2 = 12.9k\Omega$ is the quantum resistance) part which is a nonzero constant [28]. In an ideal (the barrier strength $Z = 0$) Andreev reflection process below the transition temperature T_c, the point contact resistance will drop towards half of the normal resistance according to the well-known Blonder-Tinkham-Klapwijk (BTK) theory [29]. In a nonideal situation ($Z > 0$), the tunneling process should be considered and the resistance at zero bias will go up with decreasing temperature at low temperatures [21], which is consistent with our observation of the resistance upturn below 1.3 K at zero field. The transition temperature of 3.0 K (T_c^{onset} of PC) is close to the maximum T_c^{onset} (2.8 K) of TaP under the pressure of 30 GPa [14] in a previous work, further confirming the detection of superconductivity by tip point contact measurements. The spectra in Figs. 1(c) and 1(d) show a characteristic double-peak structure and two broad conductance dips. These two structures are both related to superconductivity as they totally disappear at the T_c^{onset} 3.0 K [see Fig. 1(c)] or critical field around 3 T at 0.5 K [see Fig. 1(d)]. The existance of the characteristic double-peak feature ensures that this point contact state is in the ballistic or diffusive regime where the energy information of superconductivity gap can be resolved [21]. The spectra in other regimes can be seen in Fig. S5 and S6 in the Supplemental Material [30] (SM) . The spectra in Fig. 1(c) cannot be well explained by the s-wave BTK model [29] and the fitting results give the ratio $2\Delta/k_BT_c$ is 1.93, which is not reasonable since it is much smaller than the Bardeen-Cooper-Schrieffer weak coupling limit of 3.53 (see the SM [30]). Therefore, other pairing symmetry components should be considered in the TISC of inversion-symmetry-broken Weyl semimetal TaP. Since singlet and triplet pairings are always mixed in the wave function of the Cooper pairs in superconductors without inversion symmetry [31], the deviation of the $2\Delta/k_BT_c$ ratio can be attributed to the triplet pairing component. The double conductance peaks feature can be explained by the nonzero energy ABS at the in-plane tunneling condition for the anistropic superconductors [32–34].

For conventional superconductors, the singlet pairing Cooper pairs can be broken by ferromagnetism while the triplet pairing Cooper pairs in unconventional superconductors can stand against ferromagnetism. Since TaP is noncentrosymmetric, the spin-orbit interactions would lead to unconventional parity mixing of spin-triplet and spin-singlet Cooper pairs in the TISC. Thus, in order to ensure the unconventional component of the TISC, a ferromagnetic Ni tip is used on the topological Weyl semimetal TaP single crystal. Interestingly, the superconductivity induced at the interface of Ni-TaP structure is not suppressed by the ferromagnetism but shows the T_c^{onset} [5.8 K, Ni tip, Fig. 2(a), S7] even higher than those with a normal tip (1.0–3.0 K, PtIr or Au tip, Fig. S2–S6).

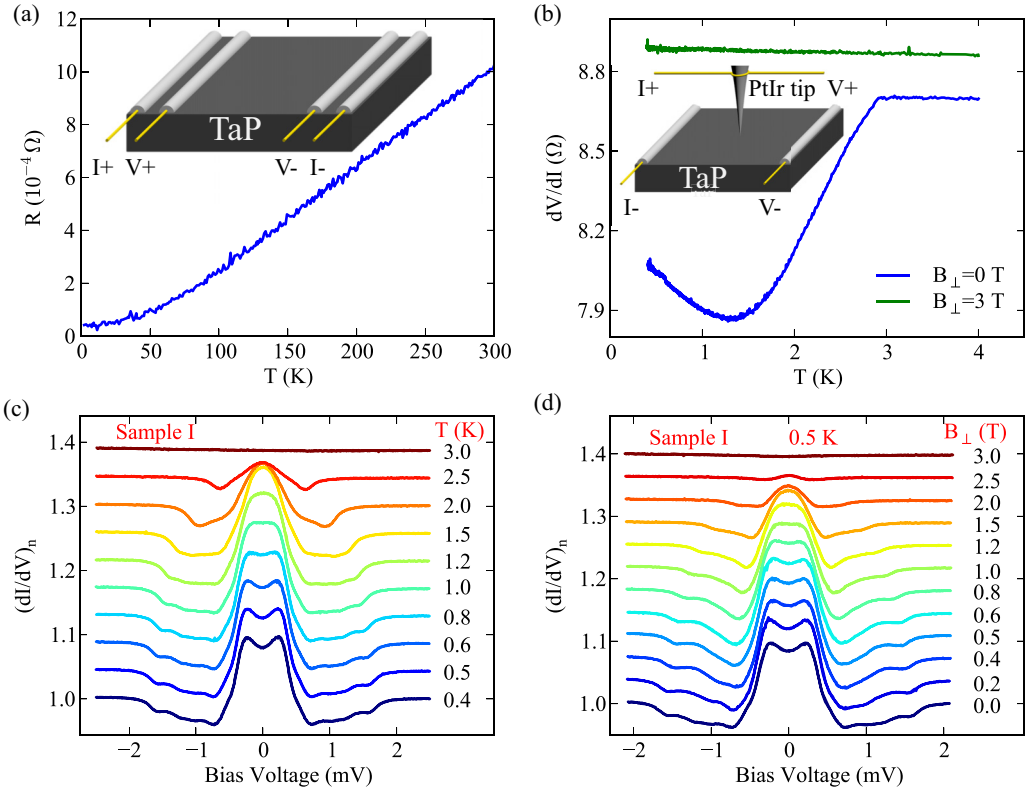

FIG. 1. Superconducting features with a T_c^{onset} of 3.0 K in Sample I at a PC resistance of 8.6 Ω with PtIr tip. (a) The temperature dependence of the standard four-electrode resistance of S1 at zero field (blue curve). (b) PC resistance versus temperature of S1, showing an T_c^{onset} of 3.0 K. (c) Normalized *dI/dV* spectra for the temperature range from 0.4 to 3.0 K. (d) Normalized *dI/dV* spectra at 0.5 K under different out-of-plane magnetic fields. Proper shift has been made in (c) and (d) for clarity.

A statistic result of the superconducting critical temperature T_c with different types of tips can be seen in Fig. 2(b). Note that the highest T_c in high-pressure measurements can only be 2.8 K [14], which is consistent with the PC results of nonferromagnetic tips, the nearly twice enhancement of T_c with the ferromagnetic Ni tip should be due to the broken time reversal symmetry of the tip, suggesting a *p*-wave component in the pairing symmetry. The representative spectra with the double conductance peaks feature are shown in Fig. 2(c) and 2(d). The gap energy of TISC on TaP is estimated to be 1.1 mV by the location of the double-peak feature at 0.6 K in Fig. 2(c). The spectra at different temperatures cannot be fitted by the spin-polarized *s*-wave BTK model if the fitting parameters of the barrier strength Z and the spin polarization P are fixed to constants, showing the deviation from the simple *s*-wave scenario. Therefore, our PCS results from both nonmagnetic and ferromagnetic tips suggest the unconventional superconductivity on the surface of the noncentrosymmetric Weyl semimetal TaP.

It is also important to see if any structural phase transitions (SPTs) happen under the tip since SPTs together with induced superconductivity are observed in many topological materials [14,35–37] with high pressure measurements. Although, the T_c values of TaP from high pressure measurements and the point contact with nonmagnetic tips are close, which means two methods may show similar mechanism on inducing the superconductivity. However, the pressure exerted by the tip is impossible to be as high as 30 GPa and the carrier doping effect between the tip and surface should also contribute to the tip-induced superconductivity. We can estimate the pressure in terms of the tensile strength of the different tips since tensile strength describes the maximum stress that a material can handle before breaking. The tensile strengths of PtIr alloy, tungsten, gold, and nickel are 1.5, 1.92, 0.22, and 0.66 GPa, respectively. Thus, the maximum pressure exerted by the tip is smaller than 1.92 GPa. The SPT is not likely to occur under such a small pressure, which can be supported by comparing the Shubnikov–de Haas (SdH) oscillations results between the traditional four-electrode transport measurements and our PC measurements. By traditional four-electrode transport measurement, the SdH oscillations are observed below 50 K. The $MR(R(B)/R(B=0T))$ is around 2000 at 2.1 K [see Fig. 3(a)] with perpendicular external field ($B//c$ axis), confirming the high quality of our TaP single crystal [11]. A major frequency $F = 18.6$ T is obtained through Fourier transformation after subtracting a polynomial background from the original data at 2.1 K, together with the second harmonics $2F = 37.2$ T peak [see lower inset of Fig. 3(b)], likely due to Zeeman splitting. The linear fitting of the Landau index n with respect to $1/B$ intercepts around zero [see upper inset of Fig. 3(b)], suggesting the π Berry's phase of TaP band structure due to the existence of Weyl points. Interestingly, the obvious SdH oscillations are also observed in our PC measurements but with the major frequency 25.5 T [see upper inset of Fig. 3(c)]. These two frequencies of 18.6 and 25.5 T show correspondence to the reported hole pockets $F_\beta = 18$ T and $F_\gamma = 25$ T [10]. The

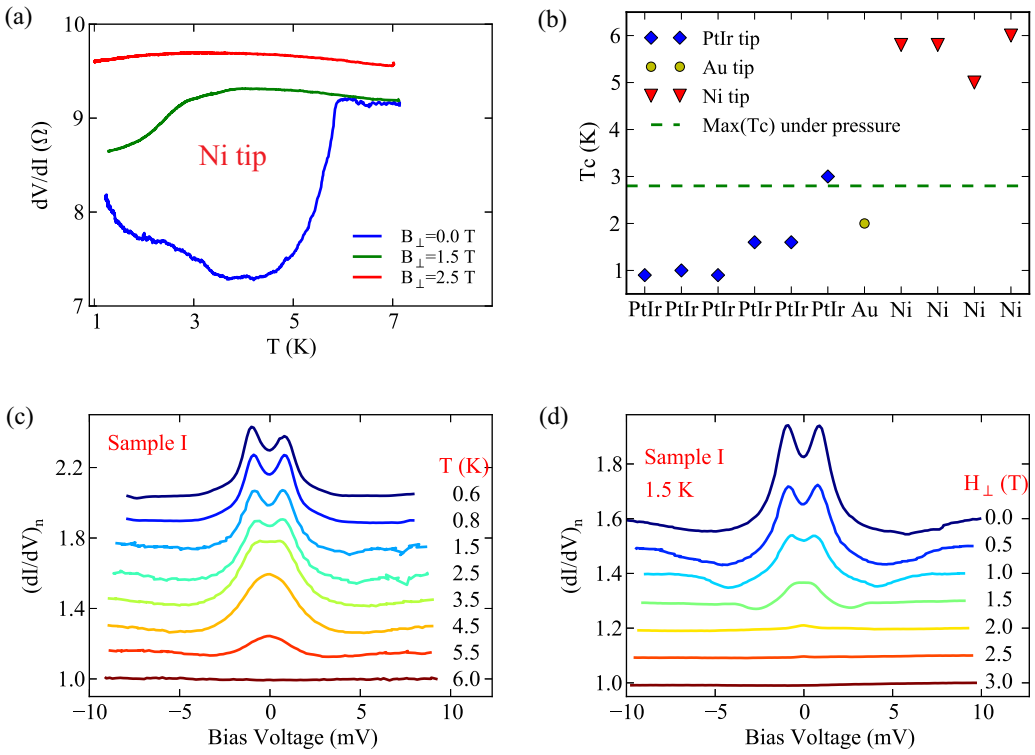

FIG. 2. Superconducting features with a T_c^{onset} of 5.8 K in Sample I at a PC resistance of 7.3 Ω with Ni tip. (a) PC resistance versus temperature of Sample I, showing an onset T_c of 5.8 K. (b) A statistic result of the superconducting critical temperature T_c with different types of tips. (c) Normalized *dI/dV* spectra for the temperature range from 0.6 to 6.0 K. (d) Normalized *dI/dV* spectra at 1.5 K under different out-of-plane magnetic fields. Proper shift has been made in (c) and (d) for clarity.

similar behavior in linear fitting of $1/B$ versus the Landau index n in the inset of Fig. 3(d) indicates that the nontrivial topological properties of the Weyl semimetal TaP still remain under our tip point contact. This is consistent with the high pressure results in which the Fermi-surface topology of TaP is proved to be robust under pressures, with the frequencies of the SdH oscillations being nearly unaffected by the pressure up to 1.7 GPa [38].

IV. DISCUSSIONS

In experiments of TISC in TaP, both the critical temperature T_c and the superconducting gap increase when a magnetic tip is employed. This very unique property strongly suggests that surface states of TaP play a major role in the TISC. Indeed, for symmetry reason, any time-reversal breaking effects should suppress a bulk superconductivity of TaP. Since TaP is noncentrosymmetric, time-reversal symmetry is the only symmetry that ensures the energy degeneracy between fermionic states with opposite momenta in three dimensions, which is necessary for the formation of bulk Cooper pairs with zero total momentum. Therefore, the time-reversal breaking due to the magnetic tip should suppress bulk superconductivity of TaP. On the other hand, surface superconductivity can be retained if the time-reversal breaking effect keeps the C_2 rotation symmetry around the c axis [39]. Actually, for the (001) surface of TaP, the C_2 rotation ensures the energy degeneracy between a surface electron with momentum $\boldsymbol{k} = (k_x, k_y)$ and that with $-\boldsymbol{k}$, which is necessary for the formation of Cooper pairs. If a tip is magnetically ordered along the c axis, the system keeps the C_2 rotation symmetry, and thus we can retain the surface superconductivity. (For details, see Part III in the SM [30].)

The theoretical deduction of the stability of the surface superconductivity under the Zeeman field is consistent with the experiments of the ferromagnetic tip-induced superconductivity in TaP. Furthermore, the experimentally detected T_c increase might be related to details of the surface state. As was shown in Ref. [40], the pairing amplitude of surface states can increase when they are well localized on the surface. Theoretically, if a Zeeman field affects the localization scale, then T_c can change.

V. CONCLUSIONS

As a conclusion, we systematically investigate the point contact spectra of the topological Weyl semimetal TaP single crystals with different type of tips at low temperatures and high magnetic fields. Superconductivity showing an unconventional nature is induced on the TaP surface by both nonmagnetic and ferromagnetic tips. Furthermore, the superconducting critical temperature is enhanced when a ferromagnetic Ni tip is employed on the noncentrosymmetric Weyl semimetal TaP crystal comparing with nonmagnetic tips, which is against the trivial superconductivity. Based on our experimental results and theoretical discussions, tip-induced Weyl surface superconductivity is suggested with the large spin-triplet mixing in the gap function.

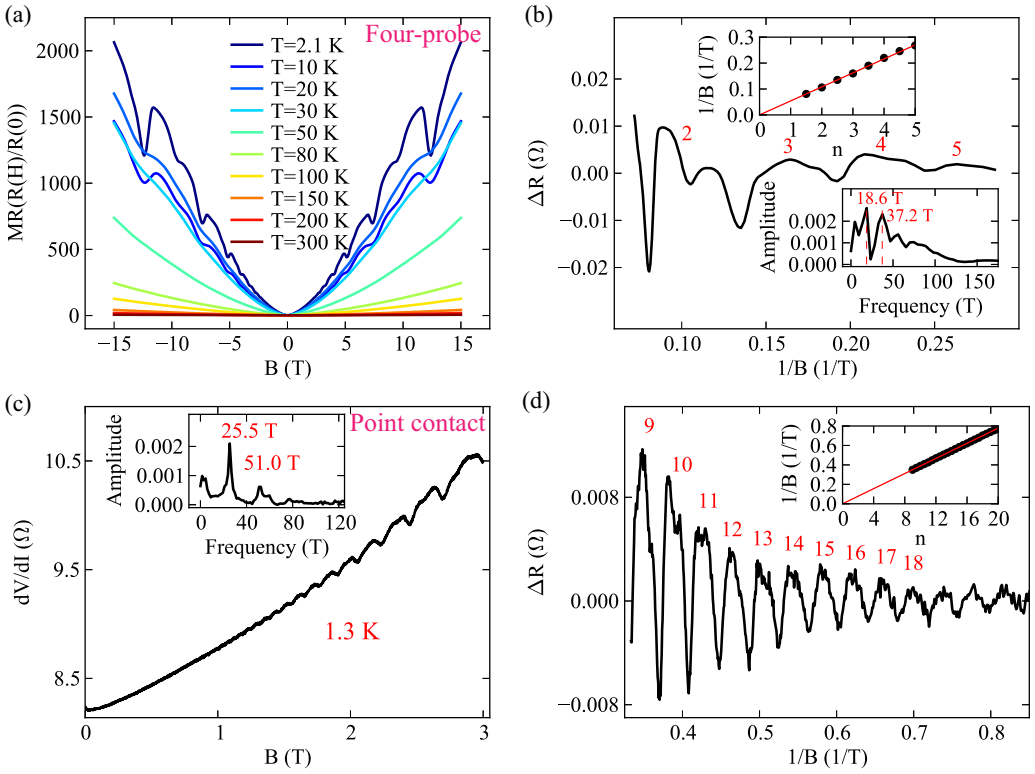

FIG. 3. Comparison of the magnetoresistance properties of TaP between four-probe transport and tip-point-contact. (a) Normalized longitudinal magnetoresistance with obvious (SdH) oscillation at selected temperatures in the perpendicular magnetic field up to 15 T by standard four-probe measurement. (b) SdH oscillation after subtracting the background from raw data at 2.1 K in (a). Lower inset: Fourier transformation of the oscillations showing peaks at $F = 18.6$ T and $2F = 37.2$ T. Higher inset: Linear fitting of the Landau fan diagram indicating a nontrivial π Berry's phase of TaP. (c) and (d) show similiar results as (a) and (b) by the point contact measurement in thermal regime. The frequency of SdH oscillation from point contact measurement is 25.5 T.

ACKNOWLEDGMENTS

We thank H. Wang, H. Ji, and J. Zhang for the help in related experiments and discussions. We thank Y. Feng for the help in sample preparation. This work was financially supported by the National Key Research and Development Program of China (2018YFA0305604 and 2017YFA0303302), the National Natural Science Foundation of China (Grants No. 11888101 and No. 11774008), the Strategic Priority Research Program of Chinese Academy of Sciences (Grant No. XDB28000000), and Beijing Natural Science Foundation (Z180010).

[1] X. Wan, A. M. Turner, A. Vishwanath, and S. Y. Savrasov, Topological semimetal and Fermi-arc surface states in the electronic structure of pyrochlore iridates, Phys. Rev. B **83**, 205101 (2011).

[2] A. A. Burkov and L. Balents, Weyl Semimetal in a Topological Insulator Multilayer, Phys. Rev. Lett. **107**, 127205 (2011).

[3] H. Weng, C. Fang, Z. Fang, B. Andrei Bernevig, and Xi Dai, Weyl Semimetal Phase in Noncentrosymmetric Transition-Metal Monophosphides, Phys. Rev. X **5**, 011029 (2015).

[4] S.-M. Huang, S.-Y. Xu, I. Belopolski, C.-C. Lee, G. Chang, BaoKaiWang, N. Alidoust, G. Bian, M. Neupane, C. Zhang, S. Jia, A. Bansil, H. Lin, and M. Zahid Hasan, A Weyl Fermion semimetal with surface Fermi arcs in the transition metal monopnictide TaAs class, Nat. Commun. **6**, 7373 (2015).

[5] S.-Y. Xu, I. Belopolski, N. Alidoust, M. Neupane, G. Bian, C. Zhang, R. Sankar, G. Chang, Z. Yuan, C.-Cheng Lee, S.-M. Huang, H. Zheng, Jie Ma, D. S. Sanchez, BaoKai Wang, A. Bansil, F. Chou, P. P. Shibayev, H. Lin, S. Jia, and M. Zahid Hasan, Discovery of a Weyl fermion semimetal and topological Fermi arcs, Science **349**, 613 (2015).

[6] B. Q. Lv, H. M. Weng, B. B. Fu, X. P. Wang, H. Miao, J. Ma, P. Richard, X. C. Huang, L. X. Zhao, G. F. Chen, Z. Fang, X. Dai, T. Qian, and H. Ding, Experimental Discovery of Weyl Semimetal TaAs, Phys. Rev. X **5**, 031013 (2015).

[7] Z. K. Liu, L. X. Yang, Y. Sun, T. Zhang, H. Peng, H. F. Yang, C. Chen, Y. Zhang, Y. F. Guo, D. Prabhakaran, M. Schmidt, Z. Hussain, S.-K. Mo, C. Felser, B. Yan, and Y. L. Chen, Evolution of the Fermi surface of Weyl semimetals in the transition metal pnictide family, Nat. Mater. **15**, 27 (2016).

[8] Y. Sun, S.-C. Wu, and B. Yan, Topological surface states and Fermi arcs of the noncentrosymmetricWeyl semimetals TaAs, TaP, NbAs, and NbP, Phys. Rev. B **92**, 115428 (2015).

[9] C. Zhang, C. Guo, H. Lu, X. Zhang, Z. Yuan, Z. Lin, J. Wang, and S. Jia, Large magnetoresistance over an extended

temperature regime in monophosphides of tantalum and niobium, Phys. Rev. B **92**, 041203(R) (2015).

[10] F. Arnold, C. Shekhar, S.-C. Wu, Y. Sun, R. Donizeth dos Reis, N. Kumar, M. Naumann, M. O. Ajeesh, M. Schmidt, A. G. Grushin, J. H. Bardarson, M. Baenitz, D. Sokolov, H. Borrmann, M. Nicklas, C. Felser, E. Hassinger, and B. Yan, Negative magnetoresistance without well-defined chirality in the Weyl semimetal TaP, Nat. Commun. **7**, 11615 (2016).

[11] C.-L. Zhang, S.-Y. Xu, C. M. Wang, Z. Lin, Z. Z. Du, C. Guo, C.-C. Lee, H. Lu, Y. Feng, S.-M. Huang, G. Chang, C.-H. Hsu, H. Liu, H. Lin, L. Li, C. Zhang, J. Zhang, X.-C. Xie, T. Neupert, M. Zahid Hasan, H.-Z. Lu, J. Wang, and S. Jia, Magnetic-tunnelling-induced Weyl node annihilation in TaP, Nat. Phys. **13**, 979 (2017).

[12] J. H. Du, H. D. Wang, Q. Chen, Q. H. Mao, R. Khan, B. J. Xu, Y. X. Zhou, Y. N. Zhang, J. H. Yang, B. Chen, C. M. Feng, and M. H. Fang, Large unsaturated positive and negative magnetoresistance in Weyl semimetal TaP, Sci. China-Phys. Mech. Astron. **59**, 657406 (2016).

[13] J. Hu, J. Y. Liu, D. Graf, S. M. A. Radmanesh, D. J. Adams, A. Chuang, Y. Wang, I. Chiorescu, J. Wei, L. Spinu, and Z. Q. Mao, π Berry phase and Zeeman splitting of Weyl semimetal TaP, Sci. Rep. **6**, 18674 (2016).

[14] Y. Li, Y. Zhou, Z. Guo, F. Han, X. Chen, P. Lu, X. Wang, C. An, Y. Zhou, J. Xing, G. Du, X. Zhu, H. Yang, J. Sun, Z. Yang, W. Yang, H.-Kwang Mao, Y. Zhang, and H.-H. Wen, Concurrence of superconductivity and structure transition in Weyl semimetal TaP under pressure, npj Quant. Mater. **2**, 66 (2017).

[15] G. Deutscher, Andreev–Saint-James reflections: A probe of cuprate superconductors, Rev. Mod. Phys. **77**, 109 (2005).

[16] F. Laube, G. Goll, H. v. Löhneysen, M. Fogelström, and F. Lichtenberg, Spin-Triplet Superconductivity in Sr_2RuO_4 Probed by Andreev Reflection, Phys. Rev. Lett. **84**, 1595 (2000).

[17] P. Szabó, P. Samuely, J. Kačmarčík, T. Klein, J. Marcus, D. Fruchart, S. Miraglia, C. Marcenat, and A. G. M. Jansen, Evidence for Two Superconducting Energy Gaps in MgB_2 by Point-Contact Spectroscopy, Phys. Rev. Lett. **87**, 137005 (2001).

[18] J. Y. T. Wei, N.-C. Yeh, D. F. Garrigus, and M. Strasik, Directional Tunneling and Andreev Reflection on $YBa_2Cu_3O_{7-\delta}$ Single Crystals: Predominance of d-Wave Pairing Symmetry Verified with the Generalized Blonder, Tinkham, and Klapwijk Theory, Phys. Rev. Lett. **81**, 2542 (1998).

[19] W. K. Park, J. L. Sarrao, J. D. Thompson, and L. H. Greene, Andreev Reflection in Heavy-Fermion Superconductors and Order Parameter Symmetry in $CeCoIn_5$, Phys. Rev. Lett. **100**, 177001 (2008).

[20] S. Sasaki, M. Kriener, K. Segawa, K. Yada, Y. Tanaka, M. Sato, and Y. Ando, Topological Superconductivity in $Cu_xBi_2Se_3$, Phys. Rev. Lett. **107**, 217001 (2011).

[21] H. Wang, L. Ma, and J. Wang, Tip-induced or enhanced superconductivity: A way to detect topological superconductivity, Sci. Bull. **63**, 1141 (2018).

[22] J. Wang, Superconductivity in topological semimetals, Nat. Sci. Rev. **6**, 199 (2019).

[23] H. Wang, H. Wang, H. Liu, H. Lu, W. Yang, S. Jia, X.-J. Liu, X. C. Xie, J. Wei, and J. Wang, Observation of superconductivity induced by a point contact on 3D Dirac semimetal Cd_3As_2 crystals, Nat. Mater. **15**, 38 (2016).

[24] L. Aggarwal, A. Gaurav, G. S. Thakur, Z. Haque, A. K. Ganguli, and G. Sheet, Unconventional superconductivity at mesoscopic point contacts on the 3D Dirac semimetal Cd_3As_2, Nat. Mater. **15**, 32 (2016).

[25] H. Wang, H. Wang, Y. Chen, J. Luo, Z. Yuan, J. Liu, Y. Wang, S. Jia, X.-J. Liu, J. Wei, and J. Wang, Discovery of tip induced unconventional superconductivity on Weyl semimetal, Sci. Bull. **62**, 425 (2017).

[26] L. Aggarwal, S. Gayen, S. Das, R. Kumar, V. Süß, C. Felser, C. Shekhar, and G. Sheet, Mesoscopic superconductivity and high spin polarization coexisting at metallic point contacts on Weyl semimetal TaAs, Nat. Commun. **8**, 13974 (2017).

[27] Y. Xing, H. Wang, C.-K. Li, X. Zhang, J. Liu, Y. Zhang, J. Luo, Z. Wang, Y. Wang, L. Ling, M. Tian, S. Jia, J. Feng, X.-J. Liu, J. Wei, and J. Wang, Superconductivity in topologically nontrivial material Au_2Pb, npj Quant. Mater. **1**, 16005 (2016).

[28] Yu. V. Sharvin, A possible method for studying Fermi surface, J. Exp. Theor. Phys. **48**, 984 (1965).

[29] G. E. Blonder, M. Tinkham, and T. M. Klapwijk, Transition from metallic to tunneling regimes in superconducting microconstrictions: Excess current, charge imbalance, and supercurrent conversion, Phys. Rev. B **25**, 4515 (1982).

[30] See Supplemental Material at http://link.aps.org/supplemental/10.1103/PhysRevMaterials.3.124201 for detailed information on the BTK analysis of Fig. 1(c), theoretical analysis of surface superconductivity and additional spectra showing tip-induced superconductivity, which includes Refs. [41–44].

[31] L. P. Gor'kov and E. I. Rashba, Superconducting 2D System with Lifted Spin Degeneracy: Mixed Singlet-Triplet State, Phys. Rev. Lett. **87**, 037004 (2001).

[32] S. Kashiwaya, H. Kashiwaya, K. Saitoh, Y. Mawatari, and Y. Tanaka, Tunneling spectroscopy of topological superconductors, Physica E **55**, 25 (2014).

[33] S. Kashiwaya, Y. Tanaka, M. Koyanagi, H. Takashima, and K. Kajimura, Origin of zero-bias conductance peaks in high-T_c superconductors, Phys. Rev. B **51**, 1350 (1995).

[34] S. Kashiwaya, H. Kashiwaya, H. Kambara, T. Furuta, H. Yaguchi, Y. Tanaka, and Y. Maeno, Edge States of Detected by in-Plane Tunneling Spectroscopy, Phys. Rev. Lett. **107**, 077003 (2011).

[35] J. L. Zhang, S. J. Zhang, H. M. Weng, W. Zhang, L. X. Yang, Q. Q. Liu, S. M. Feng, X. C. Wang, R. C. Yu, L. Z. Cao, L. Wang, W. G. Yang, H. Z. Liu, W. Y. Zhao, S. C. Zhang, X. Dai, Z. Fang, and C. Q. Jin, Pressure-induced superconductivity in topological parent compound Bi_2Te_3, Proc. Natl. Acad. Sci. **108**, 24 (2011).

[36] L. P. He, Y. T. Jia, S. J. Zhang, X. C. Hong, C. Q. Jin, and S. Y. Li, Pressure-induced superconductivity in the three-dimensional topological Dirac semimetal Cd_3As_2, npj Quantum Materials **1**, 16014 (2016).

[37] Y. Zhou, J. Wu, W. Ning, N. Li, Y. Du, X. Chen, R. Zhang, Z. Chi, X. Wang, X. Zhu, P. Lu, C. Ji, X. Wan, Z. Yang, J. Sun, W. Yang, M. Tian, Y. Zhang, and H.-k. Mao, Pressure-induced superconductivity in a three-dimensional topological material $ZrTe_5$, Proc. Natl. Acad. Sci. **113**, 2904 (2016).

[38] M. Besser, R. D. dos Reis, F.-R. Fan, M. O. Ajeesh, Y. Sun, M. Schmidt, C. Felser, and M. Nicklas, Pressure tuning of the electrical transport properties in the Weyl semimetal TaP, Phys. Rev. Mater. **3**, 044201 (2019).

[39] M. H. Fischer, M. Sigrist, and D. F. Agterberg, Superconductivity without Inversion and Time-Reversal Symmetries, Phys. Rev. Lett. **121**, 157003 (2018).

[40] T. Mizushima, A. Yamakage, M. Sato, and Y. Tanaka, Dirac-Fermion-Induced Parity Mixing in Superconducting Topological Insulators, Phys. Rev. B **90**, 184516 (2014).

[41] P. A. Frigeri, D. F. Agterberg, A. Koga, and M. Sigrist, Superconductivity without Inversion Symmetry: MnSi Versus $CePt_3Si$, Phys. Rev. Lett. **92**, 097001 (2004).

[42] M. Sigrist, D. F. Agterberg, P. A. Frigeri, N. Hayashi, R. P. Kaur, A. Koga, I. MIlat, K. Wakabayashi, and Y. Yanase, Superconductivity in noncentrosymmetric materials, J. Magn. Magn. Mater. **310**, 536 (2007).

[43] H. Q. Yuan, D. F. Agterberg, N. Hayashi, P. Badica, D. Vandervelde, K. Togano, M. Sigrist, and M. B. Salamon, *S*-Wave Spin-Triplet Order in Superconductors Without Inversion Symmetry: Li_2Pd_3B and Li_2Pt_3B, Phys. Rev. Lett. **97**, 017006 (2006).

[44] M. Sato, Y. Tanaka, K. Yada, and T. Yokoyama, Topology of Andreev bound states with flat dispersion, Phys. Rev. B **83**, 224511 (2011).